Molecular Crystals and Liquid Crystals

ISSN: 1542-1406 (Print) 1563-5287 (Online) Journal homepage: http://www.tandfonline.com/loi/gmcl20

Adsorption of a cationic water-soluble dye onto cationic Langmuir–Blodgett films via nano clay platelets: An efficient approach to control the H-dimer

J. Bhattacharjee, A. Shil, S. A. Hussain & D. Bhattacharjee

To cite this article: J. Bhattacharjee, A. Shil, S. A. Hussain & D. Bhattacharjee (2016) Adsorption of a cationic water-soluble dye onto cationic Langmuir–Blodgett films via nano clay platelets: An efficient approach to control the H-dimer, Molecular Crystals and Liquid Crystals, 624:1, 213-223, DOI: 10.1080/15421406.2015.1036508

To link to this article: http://dx.doi.org/10.1080/15421406.2015.1036508

Published online: 11 Feb 2016.

MOL. CRYST. LIQ. CRYST.
2016, VOL. 624, NO. 1, 213–223
http://dx.doi.org/10.1080/15421406.2015.1036508

Taylor & Francis
Taylor & Francis Group

Adsorption of a cationic water-soluble dye onto cationic Langmuir–Blodgett films via nano clay platelets: An efficient approach to control the H-dimer

J. Bhattacharjee, A. Shil, S. A. Hussain, and D. Bhattacharjee

Department of Physics, Tripura University, Suryamaninagar, Tripura, India

ABSTRACT

This communication reports the successful adsorption of a water-soluble cationic fluorescent dye Acridine Orange (AO) onto Langmuir–Blodgett (LB) films of a cationic amphiphile octadecylamine (ODA) in the presence of nano-clay platelets hectorite. Acridine orange (AO) has been widely used as a stainer for the characterization of biopolymers. But AO has a tendency to form non-florescent H-dimer even in the aqueous solution. Anionic nano-clay platelets hectorite played an important role in controlling the H-dimer formation of AO in the hybrid film. Effects of various parameters in the adsorption process were investigated in detail.

KEYWORDS

Anionic nano-clay platelets; AFM; cationic amphiphile; Langmuir–Blodgett film; UV–Vis; water-soluble cationic dye

Introduction

The study of dye/surfactant interaction is the source of useful information to understand several industrial processes, for example, solubilization processes to remove the organic compounds from aqueous solution and the use of surfactants to assist dying processes in textile industry [1], in photographic industries, pharmaceuticals process, etc.[2, 3]. On the other hand, adsorption is one of the promising and efficient methods of color removal [4] and also to avoid harmful by-products to treated water [5]. Recently, various groups have focused their activities on the studies of adsorption of water-soluble organic dyes [6], proteins [7–10], DNA [11–13] and other biologically important molecules and also dispersed nanoparticles [14] to mono- and multilayered Langmuir–Blodgett (LB) films. The structural characteristics such as packing and orientation of the molecules in the LB films may be changed due to adsorption. Oppositely charged molecules can easily be adsorbed onto the LB films either from solution or from the gaseous phase [5]. But adsorption of dyes onto LB films of identical charged surfactant is difficult due to the predominance of electrostatic repulsive force between the same charged molecules.

Investigations on the adsorption of various anionic organic dyes and biologically important molecules onto the cationic LB films of octadecylamine (ODA) have been reported by various research groups [15–19]. Unlike the previous works, present communication reports the adsorption process of a cationic water-soluble organic dye acridine orange (AO) onto the

CONTACT D. Bhattacharjee debu_bhat@hotmail.com Department of Physics, Tripura University, Suryamaninagar 799022, Tripura, India.
Color versions of one or more of the figures in the article can be found online at www.tandfonline.com/gmcl.

mono- and multilayered LB films of cationic surfactant ODA. Influence of anionic nano-clay platelets in the adsorption process was also studied.

Clays, such as smectite, are inorganic minerals with layered structure. They are of great interest as functional materials in the scientific field owing to their attractive properties such as appreciable surface area, ordered structure, intercalation abilities, and high ion exchange capacity [20]. They have the skill to adsorb organic materials and have shown a great promise for the construction of hybrid organic/inorganic nanomaterials. In the recent time, organo-clay hybrid film is an important area of research and has applications in different types of sensors [21–23], electrode modifiers [24–27], for modulating drug delivery [28–31], etc. Hectorite, 2:1 smectite clay, has been used as an adsorbent for the removal of cationic dyes and metal ions [32].

In the present work, cationic water-soluble dye, acridine orange (AO) has been chosen due to its key role in a wide variety of biochemical processes such as a potential sensitizing agent inducing photochemical reactions in biological environment. Various researchers have focused on the studies of the cationic behavior of acridine orange in solution and interaction with synthetic and biological systems [33]. These planar heterocyclic aromatic compounds are used as fluorescence dyes in molecular biology, biochemistry, toxicology and supramolecular chemistry [34] and stainer for the characterization of biopolymers [35]. In solution at higher concentration, AO forms aggregates leading to the formation of H-dimer [36]. Dimeric sites increase when AO is adsorbed onto solid substrate [37]. H-dimer relaxes non-radiatively from the excited state to lower excited state resulting forbidden fluorescence. H-dimer reduces the AO efficiency as a photosensitizer or fluorescent probe due to the reduction of the lifetimes and quantum yields of its electronic excited states [38]. Therefore, controlling of H-dimer has immense significance from the point of view of application as fluorescent dye and stainer in biology and for various other technological applications. One of our previous papers reported the controlling of H-dimer of AO in the presence of clay in the restricted geometry of the PAH LbL film [37]. However, controlling of H-dimer of AO onto solid substrate by using various other methods is a challenging job.

As mentioned above, the adsorption process of a cationic water-soluble organic dye acridine orange (AO) onto the mono- and multi-layered LB films of cationic surfactant ODA has been investigated. In addition, the present work also emphasizes on the controlling of H-dimeric sites of AO adsorbed onto ODA LB film using nano-clay platelets as mediator. Being highly organized in the mono- and multilayered LB films, the ionic surfactant may have the added advantage in controlling the H-dimer formation of AO molecules during the adsorption process. Detailed investigations have been carried out to study the effect of various parameters in controlling the H-dimer of AO molecules in the adsorbed film.

UV-Vis absorption spectroscopy was employed to characterize the spectroscopic properties of the AO adsorbed hybrid films. The surface morphology of the ODA–clay–AO monolayer film has been characterized by using the intermittent contact (tapping) mode AFM (atomic force microscopy).

Experimental details

Chemicals

Acridine orange (AO) ($M_w = 301.8$), purity > 99%, octadecyl amine (ODA) ($M_w = 269.51$), purity >99%, poly(allylamine hydrochloride) (PAH), purity >99% were purchased from

Sigma Aldrich Chemical Co., India and were used as received. The clay mineral hectorite used in this study was obtained from the Source Clays Repository of the Clay Minerals Society.

Methods

In order to obtain Langmuir films at the air–water interface, a small amount of the dilute chloroform solution of ODA was spread at the air–water interface of the LB trough (APEX-2000C, India) filled up with ultrapure Millipore water (18.2 MΩ cm). Allowing 30 min waiting time, the barrier was compressed at a rate of 2×10^{-3} nm^2 mol^{-1} s^{-1} to record the surface pressure–area per molecule isotherm. LB films of ODA were prepared on clean quartz substrates by dipping and rising vertically through the floating Langmuir monolayer at the air–water interface, with a speed of 5 mm/min at a fixed surface pressure of 20 mN/m to prepare mono- and multilayered LB films. The transfer ratio was found to be 0.98 ± 0.02.

Electrolytic deposition bath of cationic dye AO was prepared with aqueous solution (10^{-3} M and 10^{-4} M) using triple distilled deionized (electrical resistivity 18.2 MΩ cm) millipore water. Previously prepared LB films of ODA was then dipped into cationic AO solution for 2 hr, dried and then rinsed with water to remove surplus cations attached to the surface. Thus, the adsorption processes were completed. All the adsorption procedures were carried out at room temperature (25°C).

To study the effect of clay, loading of AO was varied with the CEC percentage of hectorite. The CEC of hectorite is 0.7 meq g^{-1}. That is aqueous dispersion of 1 g/L or 1 mg/mL hectorite clay contains 0.7 mM of negative charges. Again, aqueous solution of 301.8 g/L AO contains 1 M cationic charges. Therefore, 0.21126 mg/mL AO aqueous solution contains 0.7 mM of cationic charges. In the mixed solution of AO in clay dispersion, 10% of CEC of clay means only 10% charges of clay are sufficient to neutralize the charges of all the AO molecules. Aqueous dispersion of clay was stirred for 24 hr and then kept 30 min for sonication before using it. Aqueous AO–clay mixed dispersion with different loading (10%, 20%, 30%, 40%, and 50% of CEC of clay) were prepared. The ODA LB films were then dipped into the mixed aqueous solution of AO–clay dispersion for 2 hr and sufficient time was given for drying the slides followed by rinsing in water bath for 2 min.

UV–Vis absorption spectra were recorded using a spectrophotometer (Lambda-25, Perkin-Elmer).

AFM images of ODA–clay and ODA–clay–AO hybrid monolayer films were taken in air with commercial AFM system (Bruker Innova). Clay was adsorbed by electrostatic interactions into the preformed ODA Langmuir monolayer on the clay dispersed aqueous subphase. Subsequently ODA–clay Langmuir monolayer was transferred onto smooth silicon substrate at 20 mN/m surface pressure to prepare ODA–clay monolayer LB film. To prepare the hybrid film of ODA–clay–AO, the ODA–clay monolayer LB film was dipped into the dilute aqueous solution of AO (10^{-4} M) for 2 hr. The AFM image presented here was obtained in intermittent contact (tapping) mode. Typical scan area was 1×1 μm^2.

Results and discussion

UV-Vis absorption spectroscopy

To study the interactions between cationic–cationic and cationic–(anionic clay)–cationic, we have taken the absorption spectra of monolayer films of ODA–AO (1), ODA–clay –

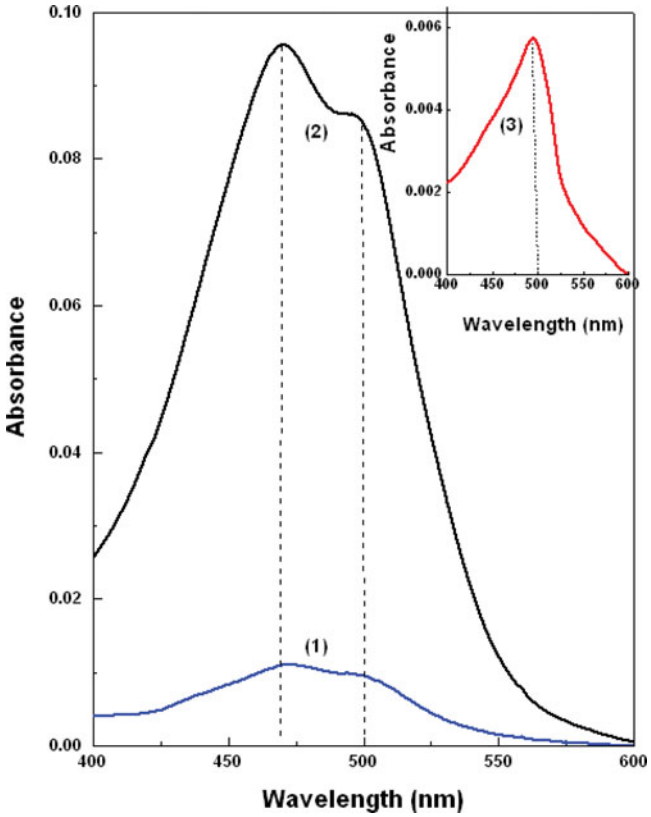

Figure 1. UV-Vis absorption spectra of (1) ODA–AO, (2) ODA–clay–AO hybrid films, the concentration of AO is 10^{-3} M and (3) ODA–clay–AO hybrid film (inset), the concentration of AO is 10^{-4} M.

AO (2) as shown in Fig. 1. The concentration of AO was 10^{-3} M and 10^{-4} M (inset of Fig. 1 (3)).

The chances of adsorption of cationic AO molecules into the cationic ODA LB monolayer was very less due to electrostatic repulsion and hence the intensity of the absorption spectrum of ODA–AO film (Fig. 1 (1)) was very weak where the concentration of AO was also comparatively higher (10^{-3} M). The strongest absorption with intense peaks was observed when cationic AO molecules were adsorbed into the cationic ODA LB monolayer using anionic nano-clay platelets as mediator. Almost ten times increase in absorbance was observed as shown in Fig. 1 (2).

It is also interesting to note from Fig. 1 that in the UV-Vis absorption spectra, two peaks are observed at 470 nm and 500 nm. The high energy band at 470 nm is due to H-dimer and 500 nm band is due to the presence of monomeric species [37]. The absorption spectrum of aqueous solution (10^{-7} M) of AO gives intense monomeric peak at 490 nm and weak H-dimer band at 470 nm (figure not shown here). With increasing solution concentration both dimeric and monomeric bands became prominent (10^{-4} M) [37]. In the AO adsorbed hybrid film, when the AO concentration was 10^{-3} M, intense dimeric band was observed and the monomeric band was reduced to a weak hump as shown in Fig. 1.

In the inset of Fig. 1, the AO concentration was 10^{-4} M. It is interesting to note that absorption spectrum of ODA–AO film was beyond the resolution. But the absorption spectrum of hybrid film of ODA–clay–AO (Fig. 1(3)) gives intense monomeric band with peak at 500 nm. Dimeric band is almost indistinguishable. It may be that at lower concentration of AO, the

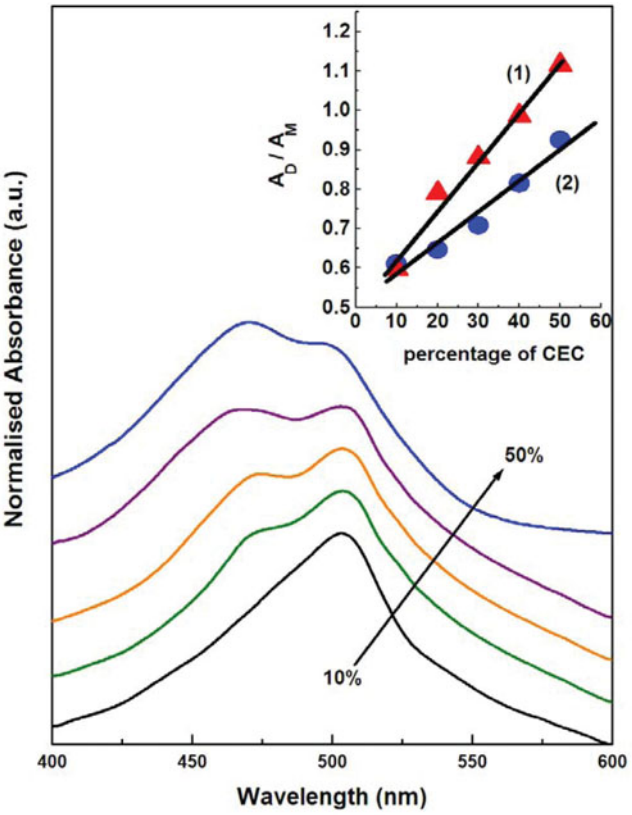

Figure 2. Normalized UV-Vis absorption spectra of AO adsorbed ODA–clay monolayer hybrid film, the loading of AO is 10%, 20%, 30%, 40%, 50% of the CEC of clay hectorite at 1 mg/mL clay in the suspension. Inset shows the variation of ratio of maximum absorbance of dimeric to monomeric band (A_D/A_M) to the change of loading percentage of CEC of clay, graph 1 is for LB monolayer and graph 2 is for previously studied [37] LbL monolayer.

adsorption of AO molecules into the nano-clay platelets occurred in a regular manner and there was less aggregation of AO molecules on the clay platelets, resulting in the decrease of dimeric sites.

Effect of nano-clay hectorite on AO dimer in hybrid films

To further extend our investigation on the effect of nano-clay platelets on controlling the H-dimer band of AO, we have performed systematic UV-Vis absorption spectroscopic studies of ODA–clay–AO hybrid LB monolayer films at various percentage of CEC of clay. Fig. 2 shows the corresponding absorption spectra for 10% to 50% of CEC of clay concentration. It is interesting to note that at 10% of CEC concentration; only intense monomeric band at 500 nm was observed. The high-energy H-dimer band was absent. With increasing loading percentage of CEC of clay, dimeric band became visible and at higher loading of 40% and 50% of CEC of clay, the dimeric band predominated over the monomeric band. In the LbL film of AO [37], the same thing was observed with prominent monomeric band at lower loading percentage of CEC of clay. However, in the present case of adsorption of AO in the LB monolayer, the effectiveness in controlling the dimeric band with lowering of the loading percentage of CEC of clay became more prominent. Inset of Fig. 2 shows the variation of ratio of maximum

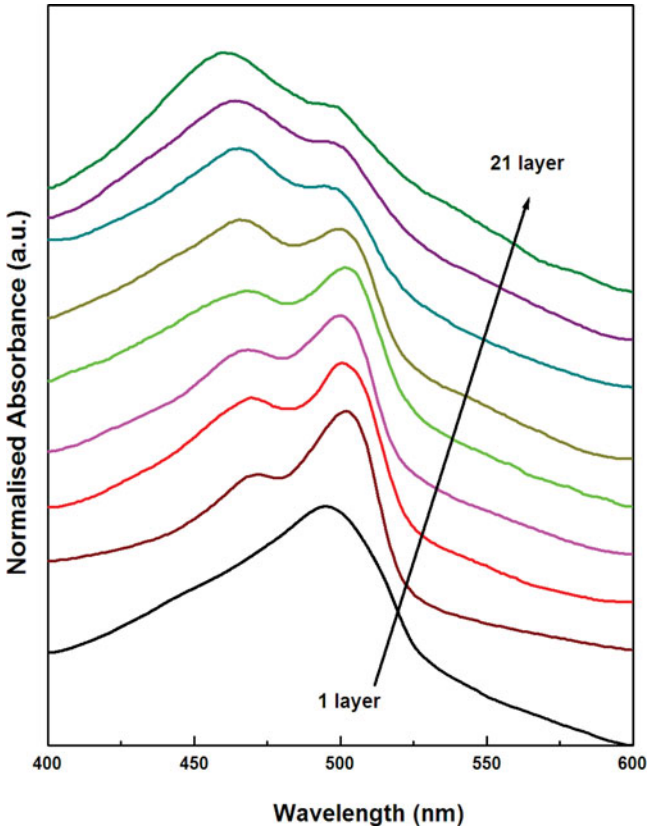

Figure 3. Normalized absorption spectra of AO absorbed onto different layered (1–21 layer) ODA LB film. In all cases, the immersion time was kept fixed at 2 hr and the AO loading is 10% of CEC of hectorite clay.

absorbance of dimeric to monomeric band (A_D/A_M) to the change of loading percentage of CEC of clay, graph 1 is for LB monolayer and graph 2 is for previously studied [37] LbL monolayer. From the figure, it is evident that in LB film, the controlling of H-dimer becomes more effective.

The most plausible explanation is that at low loading of sample, AO molecules were adsorbed onto the nano-clay platelets by cation exchange reaction [37]. It is worthwhile to mention in this context that, clay used in this work is characterized by negative charge, and it generally suppresses the aggregation of the cationic dyes [39]. Accordingly, positively charged AO molecules were arranged onto the negatively charged nano-clay platelets in a regular fashion with almost no overlapping of the AO molecules. This reduced the possibility of dimer formation and increased monomeric sites. As a result, monomeric band increased in intensity. Bujdak and Iyi [40] reported that the tendency of aggregation in the clay dispersions depends on the hydrophobic character of the dye and the properties of clay. Therefore, aggregation of the dye is expected to be low in clay dispersion resulting in intense monomeric band. Conversely, at higher loading of sample, closer association among the neighboring AO molecules took place and this was the favorable condition for H-dimer to occur.

Also unlike in the previous report [37], in the present communication, a detailed investigation has been carried out to study the effect of different parameters in the process of dimer formation. Enhancement of dimeric band has been observed in the process of adsorption of AO in the multilayer LB film.

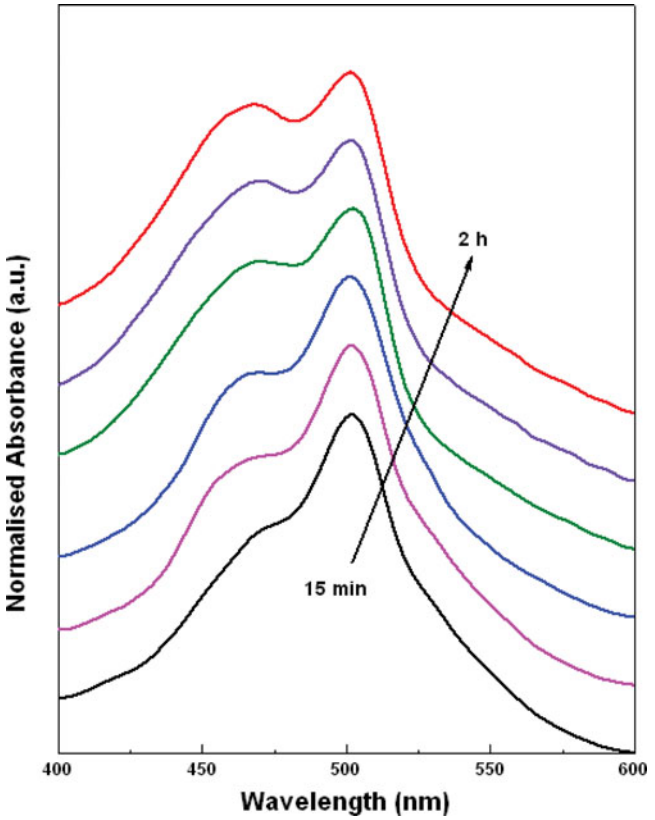

Figure 4. Normalized absorption spectra of the AO adsorbed ODA–clay hybrid film with varying immersion time from 5 min to 2 hr. Loading of AO is 10% of CEC of clay hectorite and number of layers in ODA LB film is five.

Effect of ODA layer number on AO dimer

To investigate the effect of number of layers on the dimeric sites, adsorption characteristics of AO was performed by immersing the different layered ODA LB films into the aqueous clay dispersion to AO and thus UV-Vis absorption measurement was monitored. In all the cases, the immersion time was kept fixed at 2 hr and the loading of AO is 10% of CEC of hectorite clay. Figure 3 shows the normalized absorption spectra of AO and clay adsorbed into different layered (1 — 21 layers) ODA LB film. From Fig. 2, it was clear that the dimeric sites can be controlled precisely by changing the loading of AO at 10% of CEC of hectorite clay. But from Fig. 3, it is observed that as the ODA layer number was increased; keeping the AO loading fixed at 10% of CEC of clay, the intensity of the dimeric peak at 470 nm was also increased. At higher layer number, dimeric sites predominated over the monomeric sites. The most probable explanation is that with increasing ODA layer number, larger number of AO tagged clay platelets might be squeezed, overlapped on each other, lying flat and penetrated inside the arrays of ODA molecules.

Effect of immersion time on AO dimer

Figure 4 shows the normalized absorption spectra of ODA–clay–AO hybrid films with varying immersion time from 5 min to 2 hr, the ODA layer number and the loading of

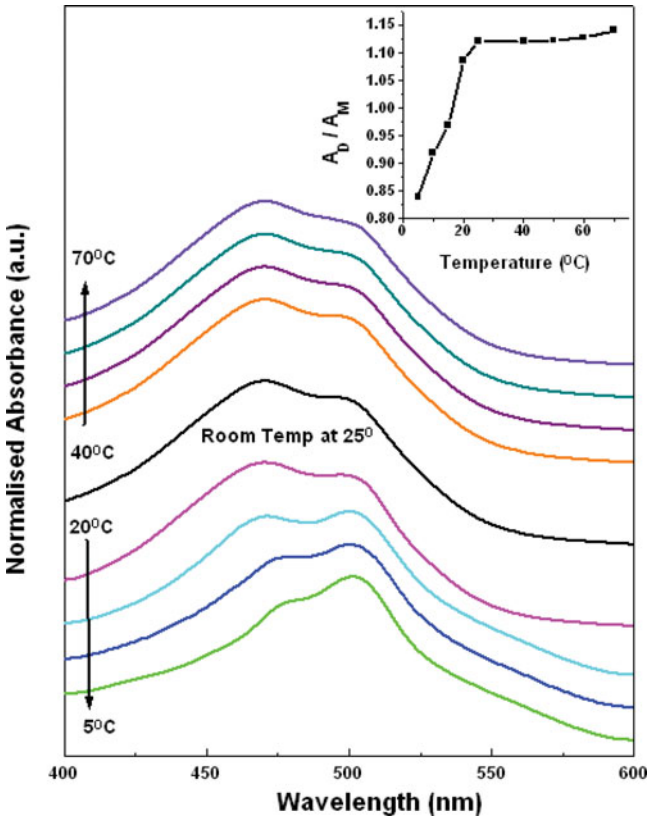

Figure 5. Normalized absorption spectra of the AO adsorbed ODA–clay hybrid film with varying temperature. Loading of AO is 50% of CEC of clay hectorite and monolayer of ODA LB film was taken. Inset shows ratio of dimer to monomer absorbance (A_D/A_M) vs. temperature.

AO were fixed at 5 layers and 10% of CEC of hectorite, respectively. It was observed that with increasing immersion time from 5 min to 2 hr, the absorbance of the dimer peak increased. It may be that with increasing immersion time, the penetration of AO tagged nanoclay platelets between the ODA layers increased resulting in the closer association of AO molecules.

Temperature effect

Figure 5 shows the effect of temperature on the ODA–clay–AO hybrid monolayer film. AO loading is 50% of CEC of clay. At normal temperature, intense dimeric band is observed. With increasing temperature, the intensity ratio of dimeric and monomeric band remains almost same. But at lower temperature, monomeric band becomes intense and at 5°C temperature dimeric band reduces to a weak hump. It may be that with decreasing temperature, atmospheric water molecules condense and get stacked among the AO molecules. As a result, dimeric sites decrease.

Aging effect

For commercial application, the stability of the film is of utmost importance. Once the monomeric band is formed in the monolayer ODA–clay–AO LbL film, it is kept for aging

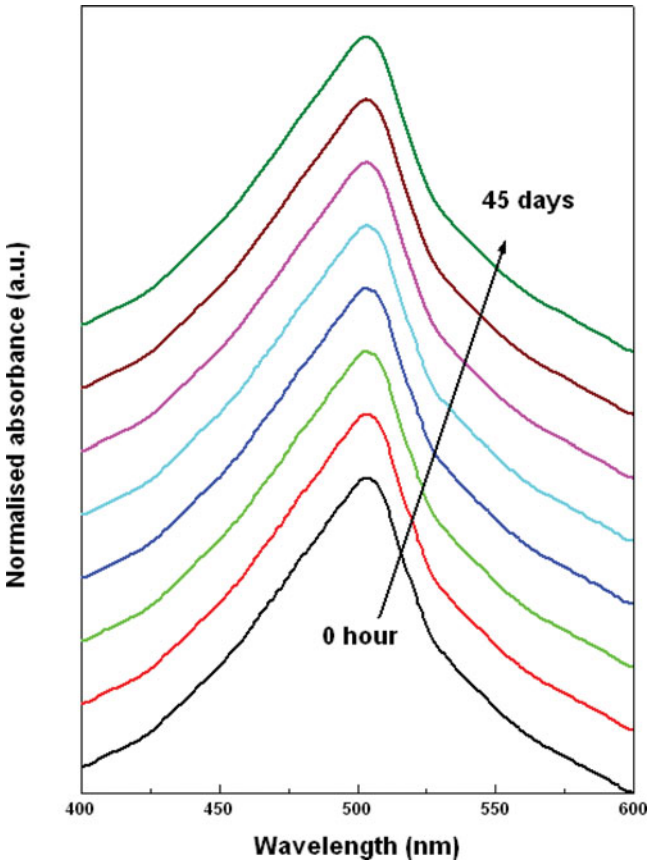

Figure 6. Normalized absorption spectra of the AO adsorbed ODA–clay hybrid film with varying aging time.

up to 45 days. No changes in the monomeric band pattern were observed as shown in Fig. 6. This certainly concludes that once the AO molecules were tagged onto the clay platelets and consequently organized onto the LbL film, they remained so and no molecular movement occurred in the ultrathin film. These films are suitable for commercial purpose.

Atomic force microscopy (AFM)

The morphology and surface structure of ODA–clay and ODA–clay–AO hybrid monolayer films deposited onto smooth Silicon wafers were studied by AFM as shown in Figs. 7(a) and (b). In the AFM image of ODA–clay hybrid film (Fig. 7(a)) the clay platelets are clearly visible. The clay particles are densely packed and cover almost the whole surface. The dimensions of ODA molecules are beyond the scope of the resolution of AFM system. However, the most interesting thing was observed in the AFM image of ODA–clay–AO hybrid monolayer film as shown in Fig. 7(b). In the AFM image, an undulating surface was observed with some linear array background. From the image, it is clear that hectorite clay platelets were first adsorbed on the ODA monolayer and then they were covered by a thin layer of AO molecules. It is as if that clay platelets were wrapped by two thin layers, one of ODA and another of AO molecules. Thus, AFM images give clear visual evidence of the formation of ODA–clay–AO hybrid film.

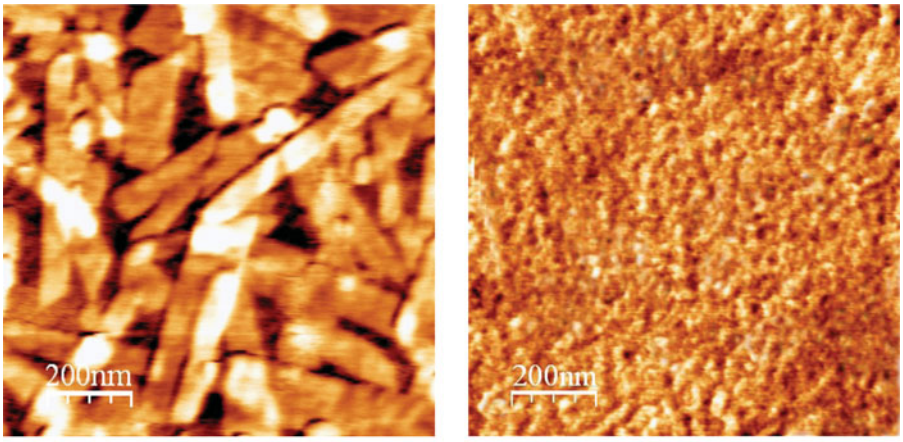

Figure 7. AFM images of (a) ODA–clay and (b) ODA–clay–AO hybrid films.

Conclusions

In conclusion, our results showed that fluorescent cationic dye AO molecules were adsorbed onto a cationic template ODA LB film via anionic nano-clay platelets hectorite and formed ODA–clay–AO hybrid film. Anionic nano-clay platelets played a vital role in controlling the H-dimer formation of AO molecules in the hybrid film. It was investigated by employing UV-Vis absorption spectroscopic technique. AFM images gave clear visual evidence of the distinct differences in ODA–clay hybrid monolayer film and AO adsorbed ODA–clay hybrid monolayer film. Aging effect study showed that once the monomeric sites of AO were formed in the film, it remained so for more than 45 days.

Acknowledgment

The author J.B. is grateful to DST for financial support to carry out this research work through Women Scientist Project (Ref. No. SR/WOS-A/PS-47/2013).

References

[1] Gul, F., Khan, A. M., Shah, S. S., & Nazar, M. F. (2010). *Coloration Tech.*, *126*, 109.
[2] Garcio-Rio, L., Hervella, P., Mejuto, J. C., & Parajo. M. (2007). *Chem. Phys.*, *335*, 164.
[3] Simomcic, B., & Kert, M. (2002). *Dyes Pigm.*, *54*, 221.
[4] Wang, Y., & Chu, W. (2011). *Ind. Eng. Chem. Res.*, *50*, 8734.
[5] Allen, S. J. (1996). *Types of Adsorbent Materials: Use of Adsorbents for Removal of Pollutants from Wastewaters*. CRC: Boca Raton, FL, USA, 59.
[6] He, C., & Hu, X. (2011). *Ind. Eng. Chem. Res.*, *50*, 14070.
[7] Hu, G., Jiao, B., Shi, X., Valle, R. P., Fan, Q., & Zuo, Y. Y. (2013). *ACS Nano.*, *7*, 10525.
[8] Guimarães, J. A., Ferraz, H. C., & Alves, T. L. M. (2014). *Appl. Surf. Sci.*, *298*, 68.
[9] Sandhya, S., Lakshmanan, M., & Dhathathreyan, A. (2008). *Appl. Surf. Sci.*, *254*, 6575.
[10] Chen, Q., Xu, S., Li, R., Liang, X., & Liu, H. (2007). *J. Colloid Interface Sci.*, *316*, 1.
[11] Hansda, C., Hussain, S.A., Bhattacharjee, D., & Paul, P.K. (2013). *Surf. Sci.*, *617*, 124.
[12] Wua, J.-C., Lina, T.-L., Jeng, U.-S., Lee, H.-Y., & Gutberlet, T. (2006). *Physica B*, *841*, 385.
[13] Fujimori, A., Taguchi, M., & Arai, S. (2014). *Colloids Surf. A*, *443*, 432.
[14] Narayanam, P. K., Srinivasa, R. S., Talwar, S. S., & Major, S. S. (2011). *Colloids Surf. A.*, *380*, 292.
[15] Takahashi, M., Kobayashi, K., & Takaoka, K. (2000). *Langmuir*, *16*, 6613.

[16] Gur, B., & Meral, K. (2012). *Colloids Surf. A*, *414*, 281.
[17] Wang, K.-H., Syu, M-J., Chang, C-H., & Lee, Y.-L. (2011). *Langmuir*, *27*, 7595.
[18] Choudhury, S., Chitra, R., & Yakhmi, J. V. (2003). *Thin Solid Films*, *440*, 240.
[19] Babenko, D. I., Ezhov, A. A., Turygin, D. S., Ivanov, V. K., Arslanov, V. V., & Kalinina, M. A. (2012). *Langmuir*, *28*, 125.
[20] Varade, D., & Haraguchi, K. (2013). *Langmuir*, *29*, 1977.
[21] Dey, D., Saha, J., Roy, A. D., Bhattacharjee, D., & Hussain, S. A. (2014*). Sens. Actuators B.*, *195*, 382.
[22] Dey, D., Bhattacharjee, D., Chakraborty, S., & Hussain, S. A. (2013). *Sens. Actuators B.*, *184*, 268.
[23] Lee, S. M., & Tiwari, D. (2012). *Appl. Clay Sci.*, *59–60*, 84.
[24] Salmi, Z., Benzarti, K., & Chehimi, M. M. (2013). *Langmuir.*, *29*, 13323.
[25] Gan, T., Hu, C., Chen, Z., & Hu, S. (2010). *J. Agric. Food Chem.*, *58*, 8942.
[26] Chang, Y., Liu, Z., Fu, Z., Wang, C., Dai, Y., Peng, R., & Hu, X. (2014). *Ind. Eng. Chem. Res.*, *53*, 38.
[27] Maghear, A., Tertiş, M., Fritea, L., Marian, I. O., Indrea, E., Walcarius, A., & Săndulescu, R. (2014). *Talanta.*, *125*, 36.
[28] Aguzzi, C., Cerezo, P., Viseras, C., & Caramella, C. (2007). *Appl. Clay Sci.*, *36*, 22.
[29] Oliveira, M. J. A., Estefânia, O. S., Lúcia, M. A. B., Regina, M., Amato, V. S., Lugão, A. B., & Parra, D. F. (2014). *Radiat. Phys. Chem.*, *94*, 194.
[30] Viseras, C., Cerezo, P., Sanchez, R., Salcedo, I. & Aguzzi, C. (2010). *Appl. Clay Sci., 48*, 291.
[31] Datta, M. (2013). *Appl. Clay Sci.*, *80–81*, 85.
[32] Xia, C., Jing, Y., Jia, Y., Yue, D., Ma, J., & Yin, X. (2011). *Desalination*, *265*, 81.
[33] Ulman A. (1991). An Introduction to Ultrathin Organic Films: From Langmuir–Blodgett to Self-assembly, Academic Press: New York
[34] Lagutschenkev, A., & Dopfer, O. (2011). *J. Mol. Spectrosc.*, *268*, 66.
[35] Ito, F., Kakiuchi, T., & Nagamura, T. (2007*). J. Phys. Chem. C*, *111*, 6983.
[36] Wang, F., Yang, J., Wu, X., Wang, X., Guo1, C., & Jia1, Z. (2006). *J. Lumin.*, *21*, 186.
[37] Bhattacharjee, J., Hussain, S. A., & Bhattacharjee, D. (2013). *Spectrochim. Acta Part A*, *116*, 148.
[38] Tsukamoto, T., Shimada, T., & Takagi, S. (2013). *J. Phys. Chem. A*, *117*, 7823.
[39] Bujdak, J., & Komadel, P. (1997). *J. Phys. Chem. B*, *101*, 9065.
[40] Bujdak, J., & Iyi, N. (2005). *J. Phys. Chem. B*, *109*, 4608.